UDK 528:004.352:520.8.07
Review / Pregledni znanstveni članak

Spatial Calibration of the Hyperspectral Line Scanner by the Bundle Block Adjusting Method

Vanja MILJKOVIĆ, Dubravko GAJSKI, Ela VELA – Zagreb[1]

ABSTRACT. Close-range hyperspectral imaging of objects encompasses the collection and processing of the spectral characteristics of the reflected electromagnetic (EM) radiation from object's surface at such distances from the sensor that they cannot be considered to be at optical infinity. Hyperspectral sensors used in close-range imaging applications are primarily calibrated in the spectral domain while their spatial calibration is questionable or not implemented at all. Data obtained by hyperspectral scanners are widely used, however, unlike most commonly used handheld spectrometers, the calibrated line scanner, besides the high-quality spectral data, poses the big potential in providing the accurate spatial information, too. To geolocate the spectral information gathered by the sensor, the mathematical model of the imaging the scene to image plane has to be derived and implemented, taking into consideration the expected systematic errors that influence the measuring results. That's why in this paper a new algorithm for calibrating the push-broom line scanner is derived and presented. The testing was done by hyperspectral line scanner ImSpector V9 + PixelFly.

Keywords: close-range photogrammetry, spatial calibration, hyperspectral line scanner.

1. Introduction

Hyperspectrèal imaging is the process of capturing the spectral characteristics of EM radiation reflected from an object in a wide band of electromagnetic spectrum. Each object's surface has its spectral signature. Collecting and recording the reflected radiance from the objects at different wavelengths makes it possible to discover and characterise the material from which it is built. In archaeological applications, it can support the dating techniques to locate the object on time-line chronologically. Hyperspectral scanners are part of modern progressive

[1] Dr. Sc. Vanja Miljković, Faculty of Geodesy, University of Zagreb, Kačićeva 26, HR-10000 Zagreb, Croatia, e-mail: vmiljkovic@geof.hr,

Assist. Prof. Dr. Dubravko Gajski, Faculty of Geodesy, University of Zagreb, Kačićeva 26, HR-10000 Zagreb, Croatia, e-mail: dgajski@geof.hr,

Dr. Sc. Ela Vela, Faculty of Geodesy, University of Zagreb, Kačićeva 26, HR-10000 Zagreb, Croatia, e-mail: evela@geof.hr.

technologies that enable objective and accurate information about objects. They are widely used, especially in the field of ecology, spatial planning, agriculture, pharmacy, forestry, forensics, medicine, art, archaeology, and similar (Carvalhal et al. 2005, Mewes 2010, Manoharan et al. 2015, Painter et al. 2016). Beside this, hyperspectral images allow a "look" underneath the colour of an artwork and can thus determine their authenticity or support its restoration (Kubik 2010). The presented calibration algorithm is developed for a line scanner used at distances to an object, where cannot be considered that the object resides to optical infinity. The investigations were carried out using the hyperspectral line scanner ImSpector V9 + PixelFly.

2. Hyperspectral scanners

Depending on the configuration of the sensor there are three different scanning principles. The simplest is the whisk-broom scanning principle. The object is scanned in pixel-by-pixel sequences. The image is recorded in two steps – one in the spectral and the other in the spatial domain. The scanning mechanism is necessary to collect hyperspectral data over the object's surface.

The next principle is a line scanning (Pushbroom) that captures the full spectrum of reflected EM-radiation, line by line. The scanning mechanism is not needed if sensor or object is moving during scanning. However, the accurate position of projection centre and orientation of the optical axis of the sensor is necessary, to geocode the hyperspectral data with satisfying accuracy.

The recent and the best, but most expensive and most complicated principle, is the wavelength scanning. The hyperspectral image consists of spectral channels captured as 2D image matrix. The scanning mechanism isn't needed anymore, and thus there is not present bad impact of imperfections of scanning mechanism on imaging geometry. The imaging geometry follows the formulation of perspective projection for both its dimensions.

3. Hyperspectral Line Scanners

Line scanners record one spatial and one spectral dimension, meaning that they record one row of pixels. By geocoding the lines in the spatial domain, a 2D orthorectified image is obtained. The spectral information are grouped in spectral channels. These channels contain attribute values representing spectral reflectance of object's surface.

In the case of line scanners, the footprint of the each line of captured spectral reflectance is situated in reference coordinate system according to the elements of the inner and outer orientation of the hyperspectral sensor. Linear scanning technology is common for air or satellite imaging, and some calibration publications of such cameras refer to this.

Spatial calibration of the push-broom line scanners in the close-range application was dealt with by a few authors, almost exclusively for industrial needs.

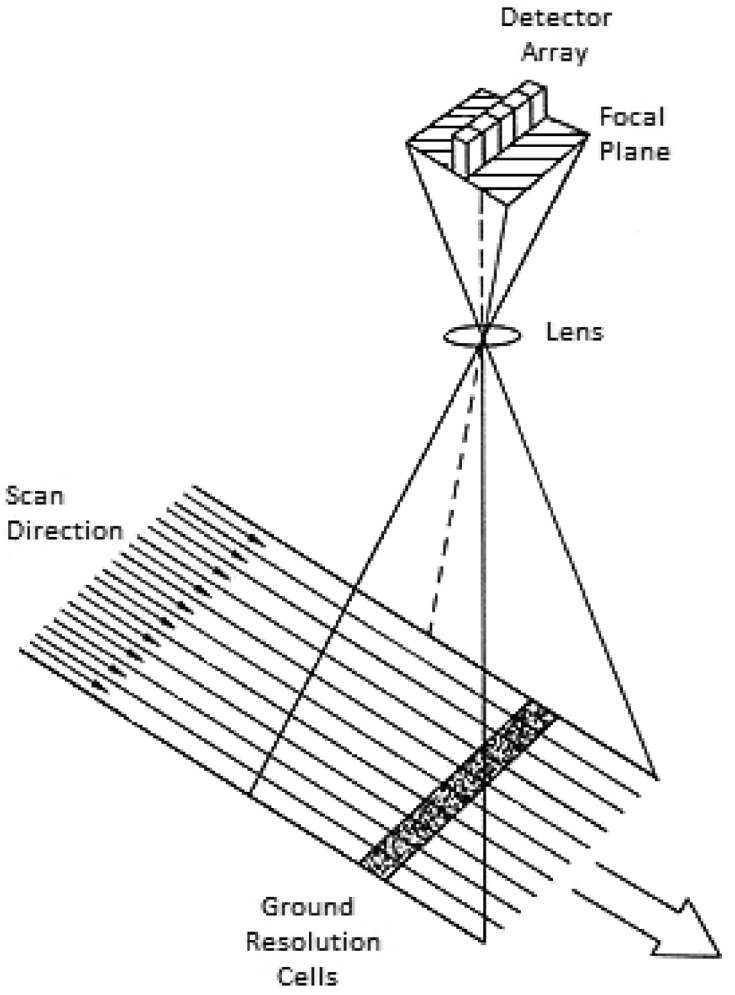

Figure 1. *The imaging geometry of the hyperspectral line scanner (URL 1).*

Zhao (2012) used a flat pattern calibration line with 58 parallel and 57 sloped lines that connect each pair of parallel lines. She linked the sample and the scanned line geometrically.

The intersections of the imaging line with the sample lines were detected, and their position was calculated based on the geometry of the sample. The calibration was performed by converting one-dimensional data into two-dimensional ones, which are linearly independent. This is solved by adding another set of data that is completely identical to the original set of data and perpendicular to it. It is assumed that the distortion of the lens in the horizontal direction causes identical effects in the vertical direction. By such approach is possible to use the formulation and software adapted for common digital cameras, where both axes of the sensor represent spatial domains.

Solving equations representing the pinhole camera model and evaluating the matrix values of the calibration parameters is made following the principles of the adjustments by least squares method.

The author used the calibration results to remove radial distortion on images that were further used to analyse and assess the quality of the textile.

Luna et al. (2010) used a similar but 3D pattern that was printed on two parallel planes. Using the geometry of the samples and the imaging line of the line scanner, the 3D coordinates of the correspondent points were calculated. These points were used to obtain the inner and outer orientation parameters by the standard calibration procedure based on bundle block adjustment principle.

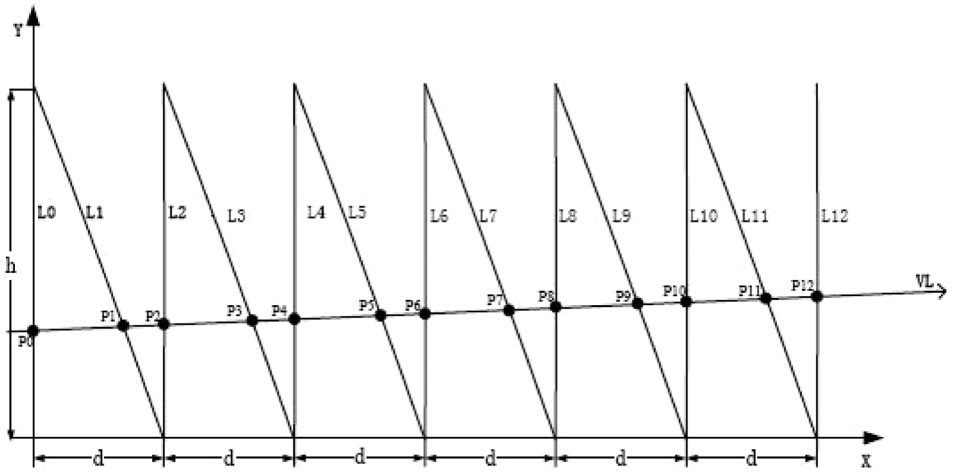

Figure 2. *Schematic representation of the sample and the imaging line (Zhao 2012).*

The method consisted of two steps. In the first step, the coordinates of intersection points are obtained at the intersections of the scan-lines with the calibration pattern. In the second step, the photo coordinates of the intersection points (calculated in the previous step) and their object coordinates were used to obtain the elements of inner and outer orientation.

The very similar calibration model was given by Li et al. (2014). The same pattern geometry was used in which, opposite to Luna et al. (2010), the calibration pattern was placed in two perpendicular planes. As in the previous example, the point coordinates of the pattern were obtained. The calibration of the multi-line push-broom sensor using the overlap area was given by Hossu and Hossu (2009). In this case, the scanner is calibrated for particularly defined industrial needs – quality control of glass on the assembly line. The system consists of two line cameras and one encoder used to measure the speed of the assembly line. The relative orientation of the assembly line to scanner lines is known and constant as well as the imaging overlap size, too.

4. Calibration of the hyperspectral line scanner ImSpector V9 + PCO PixelFly

Hyperspectral line scanner ImSpector V9 + PCO PixelFly is the sensor that records electromagnetic radiation in the visible and near-infrared spectrum (430 nm – 900 nm) It captures 24 images / sec of size: 1280x1024 pixels (horizontal (spatial) × vertical (spectral)) (Miljković and Gajski 2011). It was designed specifically for industrial and research activities.

Figure 3. *a) Hyperspectral scanner ImSpector V9, b) diffuse light collector – Phodis, c) CCD sensor PixelFly, d) Optical cable, Schneider-Kreuznach lens f = 24 mm (Bajić et al. 2004).*

The spectral measurement is done along the line to the target surface. During hyperspectral imaging the attention should be paid on that:
– the imaging line passes exactly over the surface of the sample we want to capture,
– the light source is uniformly distributed over the sample's surface, and
– the sensor's lens is focused on the sample's surface.

To satisfy the above-mentioned conditions, a black and white sample with the repetitive crown pattern was used (Figure 4).

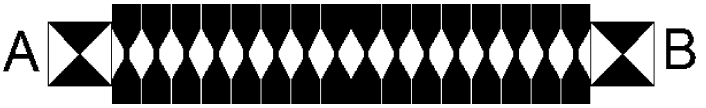

Figure 4. *Calibration pattern for ImSpector V9+PixelFly hyperspectral scanner.*

The main condition, in case of calibration of the line scanner using the given pattern, is that the scan-line corresponds with the A-B line in Figure 4. This condition is easy to fulfil by adjusting the relative orientation of the sensor towards the crown pattern. It is needed to change the rotation of sensor (or crown pattern) among all three axes to reach the thinnest and most sharp lines projected in the hyperspectral image (as seen in image 5).

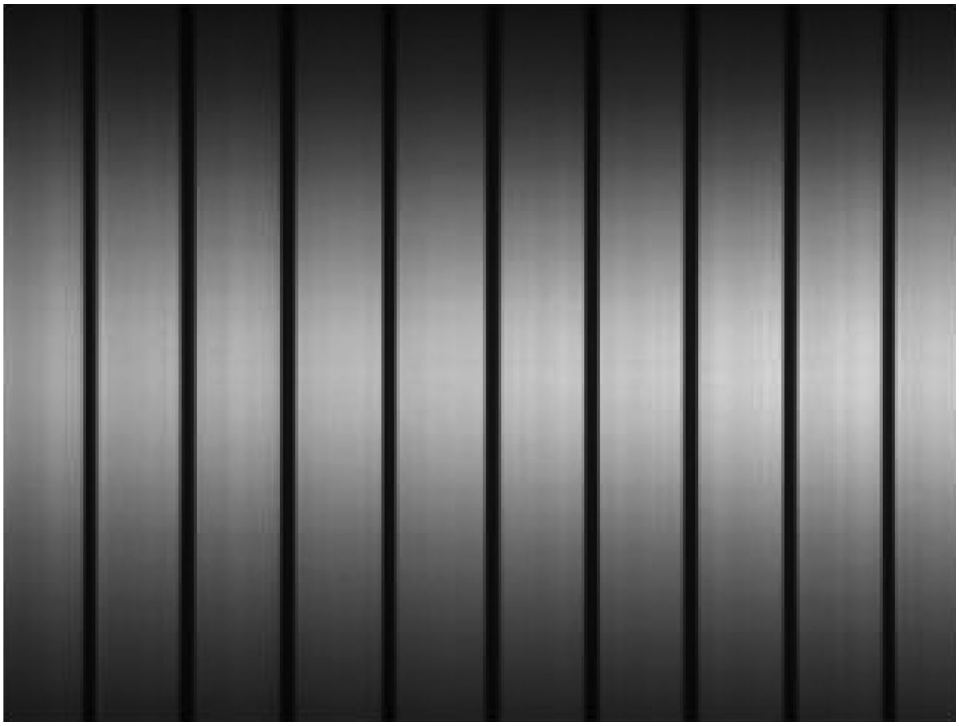

Figure 5. *A properly oriented and focused hyperspectral image towards crown pattern (Figure 4).*

A well focused and oriented hyperspectral camera produces the images showing thin and sharp vertical lines of the same thickness.

4.1. Spatial calibration of the line scanners – the proposed model

Considering the common calibration model of industrial line scanners (Chapter 3) it becomes clear that this model is adapted to industrial applications, where a fast, automated calibration on a predefined sample is required. The mathematical model follows the perspective projection of the line from the object space extended with invariant double-ratio equations. In this paper we propose the rigorous mathematical solution based on the central projection of each point from the object

space to the image plane, using the colinearity equation. Such a mathematical model is used to calibrate the digital camera with array sensors for photogrammetric purposes. In this case, the mathematical model of perspective projection uses the two-dimensional image coordinate system. Since the line scanner uses only one spatial dimension, it is necessary to set up a mathematical model and solve it in such a way that the image coordinate system is reduced to only one spatial dimension. For this purpose, the paper proposes a modified well-known Bundle block adjustment model, where the image plane degenerates to the line. Considering the imaging model of a line scanner, we first start from the assumption of an ideal (pinhole) perspective projection, whereby the auxiliary coordinate system (X', Y') is set so that the axis X' is parallel to the spatial axis of the line scanner and the axis Y' parallel to the scanning direction (Figure 6).

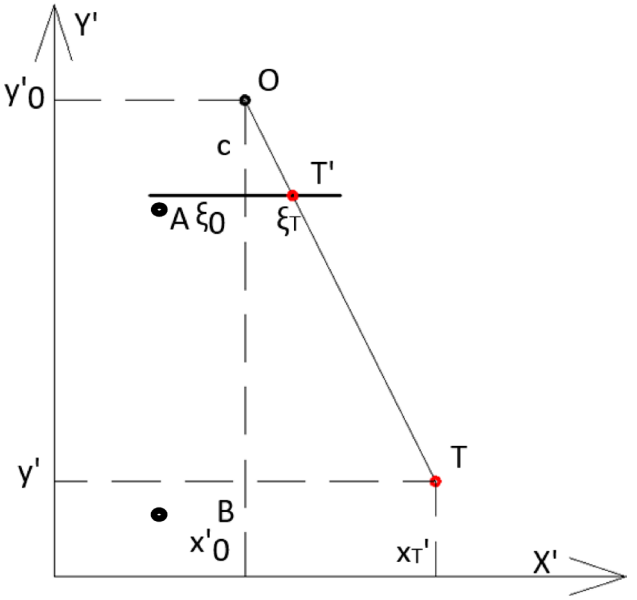

Figure 6. *The collinearity condition among the projection centre O, the point T ' and the point T.*

The colinearity condition can easily be formulated from the similarities of the triangle OT'A and OTB as follows:

$$\frac{\zeta_T - \zeta_0}{c} = -\frac{x'_T - x'_0}{y'_T - y'_0}. \tag{1}$$

The conversion of object coordinate, expressed in the auxiliary coordinate system to the reference coordinate system is done by a 2D similarity transformation, where the angle α is for the amount of positive rotation between the auxiliary and the reference coordinate system. By expanding the equation for the influence of

radial distortion (Brown 1972), a mathematical model of imaging of a line sensor is finally given:

$$\zeta_T = \zeta_0 - c\frac{(x_T - x_0)\cos\alpha + (y_T - y_0)\sin\alpha}{(y_T - y_0)\cos\alpha - (x_T - x_0)\sin\alpha} + K_1(\zeta_T - \zeta_0)^3 + K_2(\zeta_T - \zeta_0)^5 + K_3(\zeta_T - \zeta_0)^7, \quad (2)$$

where:

ζ_T – image coordinate of the measured point

ζ_0 – the position of the principal point of autocollimation (PPA) in the image coordinate system

c – the sensor's principal distance

x_T, y_T – object's reference coordinates of the measured point

α – angle of sensor's optical axis in the reference coordinate system

K_1, K_2, K_3 – radial distortion coefficients 3. 5. and 7. order.

By the linearization of the previous mathematical model (2) the observation equations for the j-point on the i-th picture are given as follows (Miljković 2017):

$$\begin{aligned} v_{\zeta\, i,j} = &\left(\frac{\partial\zeta}{\partial\zeta_0}\right)^0_{i,j} d\zeta_{0,i} + \left(\frac{\partial\zeta}{\partial c}\right)^0_{i,j} dc_i + \left(\frac{\partial\zeta}{\partial\alpha}\right)^0_{i,j} d\alpha_i + \left(\frac{\partial\zeta}{\partial x_0}\right)^0_{i,j} dx_{0,i} + \\ &+ \left(\frac{\partial\zeta}{\partial y_0}\right)^0_{i,j} dy_{0,i} + \left(\frac{\partial\zeta}{\partial \boldsymbol{x}_T}\right)^0_{i,j} dx_j + \left(\frac{\partial\zeta}{\partial y_T}\right)^0_{i,j} dy_j + \left(\frac{\partial\zeta}{\partial K_1}\right)^0_{i,j} d\boldsymbol{K}_{1,i} + \\ &+ \left(\frac{\partial\zeta}{\partial K_2}\right)^0_{i,j} dK_{2,i} + \left(\frac{\partial\zeta}{\partial K_3}\right)^0_{i,j} dK_{3,i} - \left(\zeta_{i,j} - \zeta^0_{i,j}\right) \end{aligned} \quad (3)$$

To determine the parameters of the line sensor calibration, i.e. the position of the main point (ζ_0), the camera constant (c), and the coefficients of the distortions K_1, K_2 and K_3, it is necessary to have at least five independent observations.

Beside it, the external orientation elements of the sensor according to the reference coordinate system, i.e. the position of the projection centre (x_0, y_0), and the orientation of the sensor's optical axis to the reference coordinate system (α) are not known. Therefore, for each image recorded by the same sensor, it is necessary to observe at least three new control points. The entire procedure of creating the design matrix and the observation vector as well as the adjustment according least-squares principle is programmed in SciLAB (free software similar to MatLAB).

Calibration results

Before the imaging, it was necessary to orient the camera towards the calibration pattern. To achieve this, two more signals were added on both sides of the

calibration pattern.The centre of the signal is a point that is imaged in a hyperspectral image as a very thin line, thus improving the precision of the orientation of the camera towards the calibration pattern (Figure 4).

Three images of the different camera orientation towards calibration pattern were taken, on the way that the homologous rays of photogrammetric bundles (the rays of different bundles but reflected from the same detail on the object) are intersected as close as possible to right angle (90 degrees). This ensures the favourable geometric conditions of the intersections of the homologous rays, and thus the precision of determining the elements of the inner orientation.

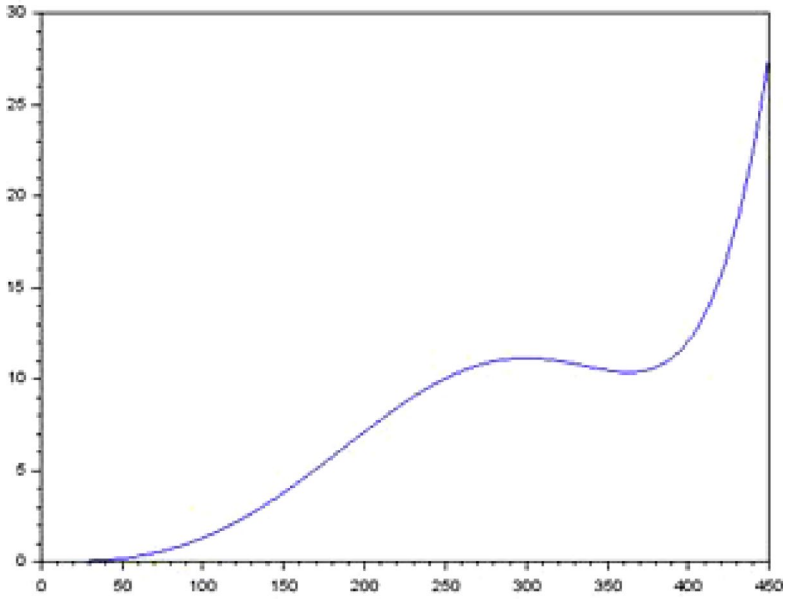

Figure 7. *Distortion values for a near-infrared spectrum (pix).*

Measurements of image coordinates on hyperspectral images were performed by tracking the changes of pixel values in the corresponding line of the image matrix (rows) for the selected wavelength. The position of the pixel in the image line, indicating the local minimum, is taken as the image coordinate of the observed point. By applying the proposed calibration procedure, the internal orientation elements for the ImSpector V9 + PixelFly hyperspectral line scanner were obtained, whereby:

K_1, K_2, K_3 – distortion coefficients 3., 5. and 7. order

x_0 – the principal point in the image coordinate system

c – principal distance.

In this case the calibration was performed for wavelength λ = 870 nm (close infra-red spectrum), the results are shown in Table 1.

Table 1. *Inner orientation elements for a near-infrared spectrum (Miljković 2017).*

	x_0 (pix)	c (pix)	K_1	K_2	K_3
uncalibrated	485	3600	0	0	0
calibrated	486.8 ± 0.1	3539 ± 14	1.459	–0.1636	0.00526

The calibration results undoubtedly point to the fact that the camera's principal distance obtained by calibration is significantly different from its assumed value. The change of the main point position is not significant about its assumed position while the radial distortion from the 200th pixel away has significant values.

Verification of the proposed spatial calibration model

As part of the TP-006/0007-01 project, MZOŠ 2008 carried out a calibration field, established at the military airport in Pula (Figure 8).

Figure 8. *Calibration field at the military airport in Pula (TP-006 2008).*

The hyperspectral imaging was performed to verify the results of parametric geocoding with the hyperspectral scanner ImSpector V9 + PixelFly CCD (HSS) functionally coupled with an inertial measuring unit iMAR iVRU-RSSC (IMU). High-precision time integration of HSS and IMU was accomplished by using precision clocks in GPS satellites. Synchronized data collection was done by the software "RECORDER", developed in the frame of technological project funded by Ministry of Science, Croatia (TP-006/0007-01).

The block diagram of the integrated system is shown in Figure 9.

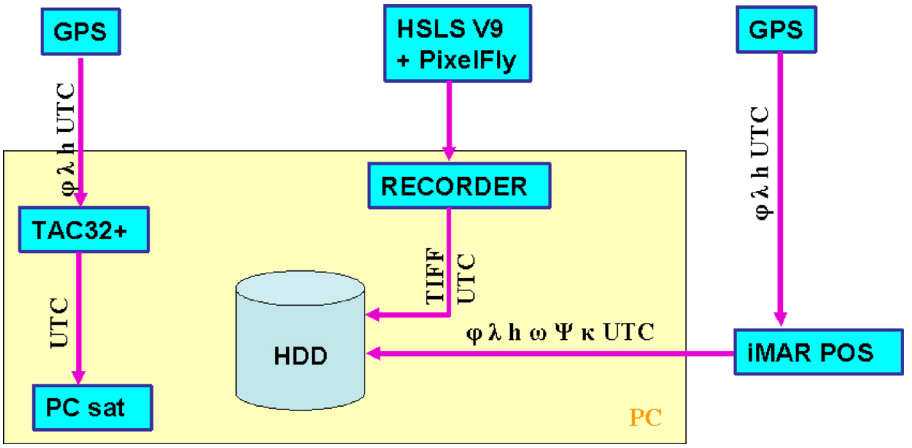

Figure 9. *Block diagram of hyperspectral imaging system built in TP-006/0007-01.*

Hyperspectral lines are approximately geocoded by use of IMU data.

The approximately geocoded hyperspectral image of the calibration field and surrounding is shown in Figure 10.

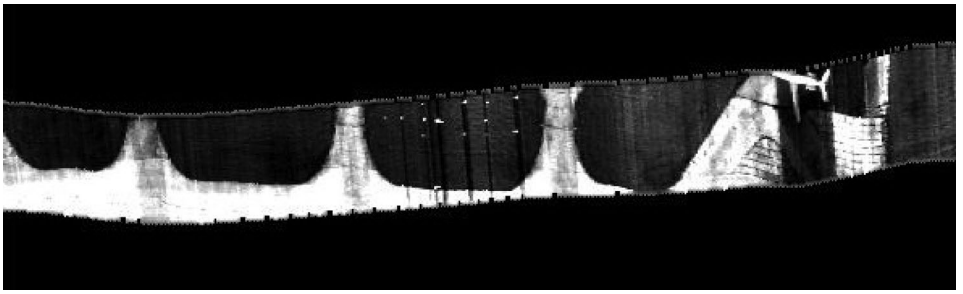

Figure 10. *Approximately geocoded one spectral channel (λ = 450 nm) taken from the hyperspectral image of the military airport (Jakšić 2009).*

As part of the graduate thesis (Jakšić 2009), geocoding of hyperspectral images was performed, using the images of the test field mentioned above. However, the hyperspectral scanner was not spatially calibrated and therefore the systematic impact of the uncalibrated hyperspectral sensor remains.

The instantaneous field of view (IFOV) was defined as the linear function of the distance from the central pixel in the sensor. The field of view was taken from the sensor specifications, and optical distortion was neglected.

Based on the model presented above, the following deviations were obtained at the control points (Figure 11).

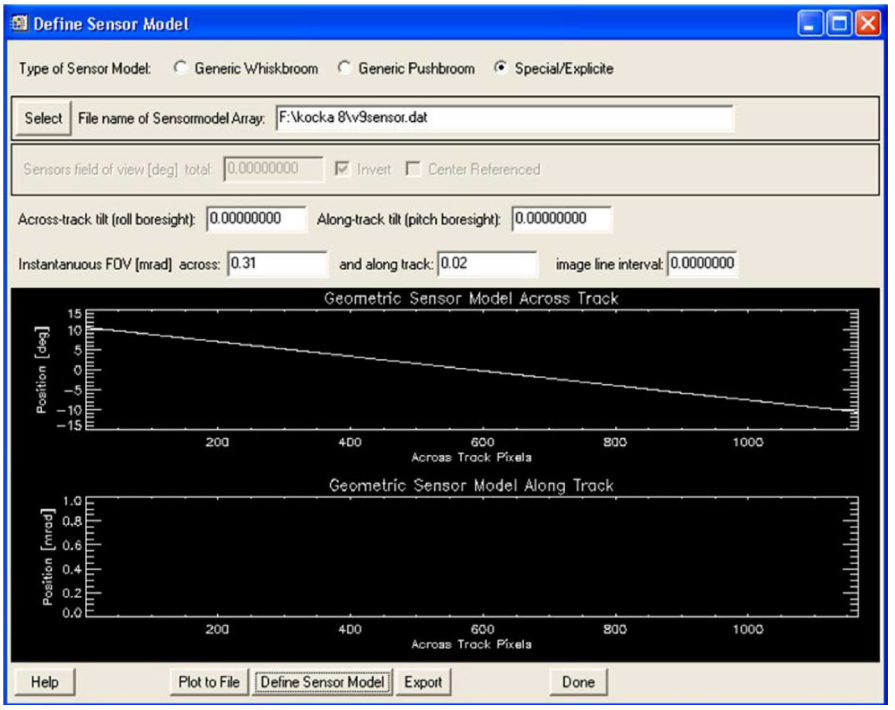

Figure 11. *Sensor model applied for parametric geocoding of the hyperspectral images as part of the TP-006/0007-01 technology project (Jakšić 2009).*

Table 2. *Deviations at control points without spatial calibration of sensors and distortions (Jakšić 2009).*

	Coordinate differences of GCP					
GCP	Δy [m]	Δx [m]	$\Delta y - n_y$	$v_y \cdot v_y$	$\Delta x - n_x$	$v_x \cdot v_x$
2	–1.1	–1.1	–0.91	0.82	–1.13	1.27
3	–1.27	0.96	–1.08	1.16	0.94	0.87
7	–0.3	0.49	–0.11	0.01	0.47	0.22
8	–0.44	0.01	–0.25	0.06	–0.02	0.00
11	–0.61	–0.25	–0.42	0.17	–0.28	0.08
12	–1.13	0.93	–0.94	0.87	0.91	0.82
16	0.34	0.32	0.54	0.29	0.30	0.09
17	0.61	–0.27	0.81	0.65	–0.30	0.09
20	1.3	–0.32	1.50	2.24	–0.35	0.12
22	0.65	–0.52	0.85	0.71	–0.55	0.30
Σ	–1.95	0.25	0.00	6.98	0.00	3.84
	bias n_y = –0.2 m	bias n_x = +0.0 m	σ_y =	0.88 m	σ_x =	0.65 m

After correction for camera's principal distance and distortion, at the control points, the following deviations were obtained (Table 3).

Table 3. *Deviations at control points using calibration and distortion elements (Miljković 2017).*

	Coordinate differences of GCP					
GCP	Δy [m]	Δx [m]	$\Delta y - n_y$	$v_y \cdot v_y$	$\Delta x - n_x$	$v_x \cdot v_x$
2	–0.31	0.21	–0.29	0.08	0.18	0.03
3	–0.58	0.33	–0.56	0.31	0.30	0.09
7	–0.36	0.45	–0.34	0.12	0.42	0.17
8	–0.44	0.15	–0.42	0.18	0.12	0.01
11	–0.26	–0.35	–0.24	0.06	–0.38	0.15
12	0.31	0.11	0.33	0.11	0.08	0.01
16	0.22	0.21	0.24	0.06	0.18	0.03
17	0.28	–0.17	0.30	0.09	–0.20	0.04
20	0.53	–0.28	0.55	0.30	–0.31	0.10
22	0.41	–0.32	0.43	0.18	–0.35	0.13
Σ	–0.20	0.34	0.00	1.49	0.00	0.75
	bias n_y = –0.02 m	bias n_x = +0.03 m	σ_y =	0.40 m	σ_x =	0.29 m

The software for parameter geocoding (PARGE) does not allow the introduction of optical distortion models to eliminate its systemic impact; it was necessary to remove the influence of the optical distortion from the observations on hyperspectral images. This is done according to a new mathematical model (formulas 1, 2 and 3). Table 3 shows a significant increase in accuracy, taking into account the spatial calibration of the sensor. A good estimation of the systematic imaging errors is also apparent in the substantial decrease in systematic impact of image coordinate errors to the final result (bias nx and bias ny are reduced to negligible size). The standard deviations of geocoded hyperspectral image evaluated in the calibration field have been reduced by more than half and provide more accurate geocoding results for the hyperspectral cube and thus better spatial accuracy in all applications using hyperspectral imaging results.

5. Conclusion

The most common approach to calibrate the line sensor in close-range applications, was to derive the calibration model using one image of 3D-pattern, specially constructed for the needed application (Luna et al. 2010). The another concept is to extend the one-dimensional imaging by one more spatial dimension (Zhao 2012). The mathematical model of imaging of linear array sensor is transformed to the mathematical model of imaging of area array sensor, for which many calibration algorithms have already been developed.

In the calibration models mentioned above, the mathematical model of the spatial calibration of the line scanner is different, comparing to the mathematical model applied in spatial photogrammetric reconstruction. In the proposed calibration model, the mathematical model of calibration corresponds to the mathematical model of spatial reconstruction (perspective projection model with additional optical distortion parameters). This enables to track and analyse the impact of calibration results on quality of spatial reconstruction. The results of the proposed calibration model were verified on the test field established at the airport in Pula. Using the parameters of inner orientation obtained by proposed calibration method in the geocoding of hyperspectral cubes shows the significant increase in positional accuracy of every geocoded pixel in the hyperspectral cube.

References

Bajić, M., Gold, H., Pračić, Ž., Vuletić, D. (2004): Airborne Sampling of the Reflectivity by the Hyper Spectral Line Scanner in a Visible and Near-Infrared Wavelengths, 24th Symposium of EARSeL, the European Association of Remote Sensing Laboratories, Dubrovnik.

Brown, D. C. (1972): Calibration of Close Range Cameras, Invited Paper, XII Congress of ISP, Ottawa, Canada Commission V, 25.

Carvalhal, J. A., Linhares, J. M. M., Nascimento, S. M. C., Regalo, M. H., Leite, M. C. V. P. (2005): Estimating the best illuminants for appreciation of art paintings, AIC Colour, 383–386.

Hossu, A., Hossu, D. (2009): Geometric and Threshold Calibration Aspects of a Multiple Line-Scan Vision System for Planar Objects Inspection, Contemporary Robotics-Challenges and Solutions, InTech, 2, 61–78.

Jakšić, J. (2009): Parametarsko geokodiranje hiperspektralnih snimki (Parametric Geocoding of Hyperspectral Images), Diploma Thesis, Faculty of Geodesy, University of Zagreb, Zagreb (in Croatian).

Kubik, M. E. (2010): Preserving the Painted Image: The Art and Science of Conservation, JAIC – Journal of the International Colour Association, 5, 1–8.

Luna, C., Mazo, M., Lázaro, J., Vázquez, J. (2010): Calibration of Line-Scan Cameras, IEEE Transactions on Instrumentation and Measurement, 59, 8, 2185–2190.

Manoharan, C., Sutharsan, P., Venkatachalapathy, R., Vasanthi, S., Dhanapandian, S., Veeramuthu, K. (2015): Spectroscopic and rock magnetic studies on some ancient Indian pottery samples, Egyptian Journal of Basic and Applied Sciences, 2, 1, 39–49.

Mewes, G. T. (2010): The impact of the spectral dimension of hyperspectral datasets on plant disease detection, Dissertation zur Erlangung des Doktorgrades Der Mathematisch-Naturwissenschaftlichen Fakultat der Rheinischen Friedrich-Wilhelms-Universitat at Bonn, Bonn.

Miljković, V. (2017): Prostorna kalibracija multispektralnih i hiperspektralnih senzora u blizupredmetnoj fotogrametriji (Spatial Calibration of Multispectral and Hyperspectral Sensors in Close-Range Photogrammetry), PhD Thesis, Faculty of Geodesy, University of Zagreb, Zagreb (in Croatian).

Miljković, V., Gajski, D. (2011): Multispectral Close-Range Facilities Survayes, In International Scientific Conference "Professional Practice and Education in Geodesy and Related Fields", Proccedings, Faculty of Civil Engineering, University of Belgrade, Belgrade, 83–88.

Painter, T. H., Berisford, D. F., Boardman, J. W., Bormann, K. J., Deems, J. S., Gehrke, F., Mattmann, C. (2016): The Airborne Snow Observatory: Fusion of scanning lidar, imaging spectrometer, and physically-based modeling for mapping snow water equivalent and snow albedo, Remote Sensing of Environment, 184, 139–152.

TP-006 (2008): System for multisensor airborne reconnaissance and surveillance in the crises situations and the protection of environment, TP-006/0007-01, Ministry of Science, Education and Sports of the Republic of Croatia, 2007–2008.

Zhao, Z. (2012): Line scan camera calibration for fabric imaging, PhD Thesis, The University of Texas at Austin, Austin.

URLs

URL 1: Lexikon der Fernerkundung, http://www.fe-lexikon.info/, (26. 1. 2017).

Prostorna kalibracija hiperspektralnoga linijskog skenera izjednačenjem zrakovnog snopa

SAŽETAK. Hiperspektralna blizupredmetna snimanja objekata obuhvaćaju prikupljanje i obradu spektralnih karakteristika reflektiranog elektromagnetskog zračenja (EM) objekata koji se nalaze na takvim udaljenostima od senzora da se ne može smatrati da se nalaze u optičkoj beskonačnosti. Hiperspektralni skeneri koji se koriste u blizupredmetnim snimanjima prvenstveno su dobro kalibrirani u spektralnoj domeni dok je njihova prostorna kalibracija upitna ili uopće nije provedena. Točkasti skeneri su najčešće korišteni hiperspektralni skeneri sa vrlo širokom upotrebom. Za razliku od točkastih skenera, kalibrirani linijski skener osim kvalitetne spektralne daje i točnu prostornu informaciju. Za geokodiranje spektralnih podataka prikupljenih senzorom potrebno je izraditi i implementirati matematički model preslikavanja scene na ravninu snimke, uzimajući u obzir očekivane sistematske pogreške koje utječu na rezultate mjerenja. Stoga je u ovom radu izveden i prezentiran novi algoritam za kalibraciju linijskih skenera. Testiranje je obavljeno pomoću hiperspektralnog linijskog skenera ImSpector V9 + PixelFly.

Ključne riječi: blizupredmetna fotogrametrija, prostorna kalibracija, hiperspektralni linijski skener.

Received / *Primljeno:* 2017-02-14

Accepted / *Prihvaćeno:* 2017-04-28